

## ULTRA-LIGHT SOL-GEL DERIVED MAGNETIC NANOSTRUCTURED MATERIALS

MIHAELA POPOVICI<sup>1</sup>, MARTI GICH<sup>2</sup>, CECILIA SAVII<sup>1</sup>

<sup>1</sup>*Institute of Chemistry Timisoara of the Romanian Academy, 24 Mihai Viteazul,  
300223 Timisoara, Romania, e-mail:mihapi@acad-icht.tm.edu.ro*

<sup>2</sup>*Institut de Ciencia de Materials de Barcelona (ICMAB-CSIC), Esfera UAB,  
08193 Bellaterra, Catalunya, Spain*

(Received March 14, 2006)

*Abstract.* Monolithic ultra-porous and ultra-light magnetic nanocomposites can be obtained by impregnating the pores of silica matrices formed by sol-gel processing, with anhydrous metal salts precursors, followed by the supercritical drying at high pressure. The crystalline phases identified by X-ray diffraction consist of metallic Ni, iron oxide spinel and Ni-ferrite, respectively.

*Key words:* sol-gel, nanocomposites, superparamagnetic behaviour.

### 1. INTRODUCTION

Magnetic particles with sizes in the nanometer scale are now of interest because of their many technological applications and unique magnetic properties which differ considerably from those of bulk materials.

Below a critical size, magnetic particles become single domain in contrast with the usual multidomain structure of the bulk magnetic materials exhibiting unique phenomena such as superparamagnetism [1] and quantum tunneling of the magnetization [2]. Magnetic nanoparticle systems exhibiting superparamagnetic behavior, display little or no remanence and coercivity while keeping a very high saturation magnetization. They have potential application in biomedicine [3-4], magnetic drug delivery and cell-sorting systems [5-6] or in magnetic refrigeration technology [7].

The confinement of nanoparticles can be achieved by using a porous matrix prepared by sol-gel process as a host. The porous amorphous matrices, within which nanostructures are developed, play an active role in determining their physical properties in addition to providing a means of particle dispersion [8]. Another important characteristic of the matrix is to act as protection of metallic

nanoparticles against air-oxidation; such is the case of metallic nickel by encapsulating them in inert matrices as graphite [9], fullerene [10] or in oxide-type matrices like zeolites [11], alumina [12-13][238], titanium dioxide [14] or silica ones [15].

Magnetic nanoparticles of Ni-ferrite have been produced in a variety of matrix materials like polystyrene [16], or silica [17], for instance.

Usually, the metal cationic species are embedded inside the pores of the silica polymeric matrix, either by *in situ* sol-gel synthesis [18] or by impregnation of mesoporous silica gels [19], in both cases using as precursors and/or desired metal salts. The resulted silica gels obtained by sol-gel hydrolysis-condensation reactions are highly porous. To preserve the high porosity, supercritical evacuation of the solvent contained in the pores is employed, in order to avoid the collapsing of gel pores. The resulted materials, named *aerogels*, are characterized by low density, very high surface area, low refractive index and low sound velocity [20]. It was reported that after supercritical drying, the resulted aerogels contain ionic or amorphous species [21], and usually to obtain the targeted metallic or oxide phases, a subsequent controlled thermal treatment often at high temperatures (500-1000°C) was required [22].

Despite the growing interest in magnetic nanoparticles, by literature survey, relatively few studies concerning aerogel nanocomposites magnetic behaviour [21, 23-30] were found. Iron oxide nanoparticles systems particularly present interesting properties with applications in several fields [31-35].

Recently, we have reported a study regarding the synthesis and characterization of iron oxide/silica aerogels with superparamagnetic behaviour [36]. The acid catalyzed sol-gel process synthesis, and impregnation followed by supercritical drying in ethanol was used in this case.

In the present study, wet silica gels were prepared in a two step acid-base catalyzed sol-gel process, using hydrochloric acid and ammonia, respectively. Subsequently, the silica gels were impregnated with two anhydrous metal (Fe(II), Ni(II)) salts, followed by supercritical drying process. The magnetic nanocomposites were directly obtained after the supercritical drying.

## 2. EXPERIMENTAL

Silica wet gels were prepared by hydrolysis and condensation of tetraethoxysilane (TEOS) (Aldrich 98%) using two step acid-base catalyzed sol-gel process (hydrochloric acid and ammonia as catalysts, respectively). In the first step, prepolymerized tetraethoxysilane was obtained by the reaction of TEOS in the presence of a sub-stoichiometric amount of water and acid catalyst (HCl 1 M)

ethanol solution. After one month at  $-25^{\circ}\text{C}$  a viscous fluid was obtained. In the second step (basic medium) a  $0.05\text{ M NH}_3$  aqueous solution was added to the acid sol. After 48 h the gelation of the matrix samples, denoted TE1AB, occurred. Subsequently, the liquid contained in the pores of the silica gels was exchanged with ethanol. Two samples were obtained by the impregnation of silica gels using supersaturated alcoholic solutions of anhydrous Ni(II) acetylacetonate (Aldrich 95%) or anhydrous Fe(II) acetylacetonate (Aldrich 99.95%). A third type of sample was obtained by simultaneous impregnation of silica gels with both Ni(II) and Fe(II) alcoholic solutions. The impregnated gels samples are referred TE1ABNi (nickel containing gels), TE1ABFe (iron containing gels) and TE1ABNiFe (iron and nickel containing gels). Supercritical drying of the impregnated gels was realised in ethanol supercritical conditions, at  $260^{\circ}\text{C}$  and a maximum pressure of 131 bars. After three hours, at the end of the supercritical treatment, the pressure in the autoclave was carefully relieved at nearly constant temperature. The obtained aerogels were left to slowly cool down to ambient temperature. No further thermal treatment was carried out. The resulted aerogels preserved the same monolithic shape as the wet gels, but they displayed a slightly diminished volume.

The as-synthesized samples were characterized by X-ray diffraction (XRD) with a D5000 Siemens X-ray powder diffractometer using  $\text{CuK}\alpha$  incident radiation ( $\lambda = 1.5406\text{ \AA}$ ). Diffraction patterns were recorded from  $10^{\circ}$  to  $80^{\circ}$  with a step size of  $0.1^{\circ}$  and a scanning rate of 15 s per step. Transmission electron microscopy (TEM) observations were performed using a Philips CM 30 microscope operating at 300 keV. For the microscopy analyses the samples were crushed, ultrasonically dispersed in ethanol and subsequently deposited onto a copper grid. Nitrogen adsorption data were taken at 77 K using an ASAP 2000 surface area analyzer (Micromeritics Instrument Corp.) after heating the samples at  $180^{\circ}\text{C}$  under vacuum for 24 h to remove the adsorbed species. Surface area determinations were carried out following the BET (Brunauer-Emmett-Teller) method. Hysteresis loops were measured at room temperature by means of a vibrating sample magnetometer (VSM) with a maximum applied field of 1 T.

### 3. RESULTS AND DISCUSSION

The aerogel slabs obtained by impregnation method are lightweight monoliths with grey-black color (TE1ABNi sample), brownish-black color (TE1ABFe sample) and black color (TE1ABNiFe sample), respectively. The bulk density of the aerogel was determined by measuring the weight and the volume of the sample, being characterized by very low densities and high surface areas with comparable values (Table 1).

Table 1  
Summary of aerogel textural characterization

Sample	Bulk density [g/cm <sup>3</sup> ]	Surface area BET [m <sup>2</sup> /g]	Dparticles (TEM) (nm)
TE1AB (SiO <sub>2</sub> )	0.05	957	-
TE1ABNi (Ni-SiO <sub>2</sub> )	0.06	857	14 ± 2
TE1ABFe (Fe <sub>2</sub> O <sub>3</sub> /Fe <sub>3</sub> O <sub>4</sub> -SiO <sub>2</sub> )	0.06	817	8 ± 1
TE1ABNiFe (NiFe <sub>2</sub> O <sub>4</sub> -SiO <sub>2</sub> )	0.06	-	10 ± 4

In the case of silica aerogel matrix (Fig. 1a) and Ni aerogel nanocomposite sample (Fig. 1b), the both obtained N<sub>2</sub> adsorption/desorption isotherms can be associated to Type IV [37], indicating that the porous structure (Fig. 1c and Fig. 1d) is mainly situated in the mesoporous range.

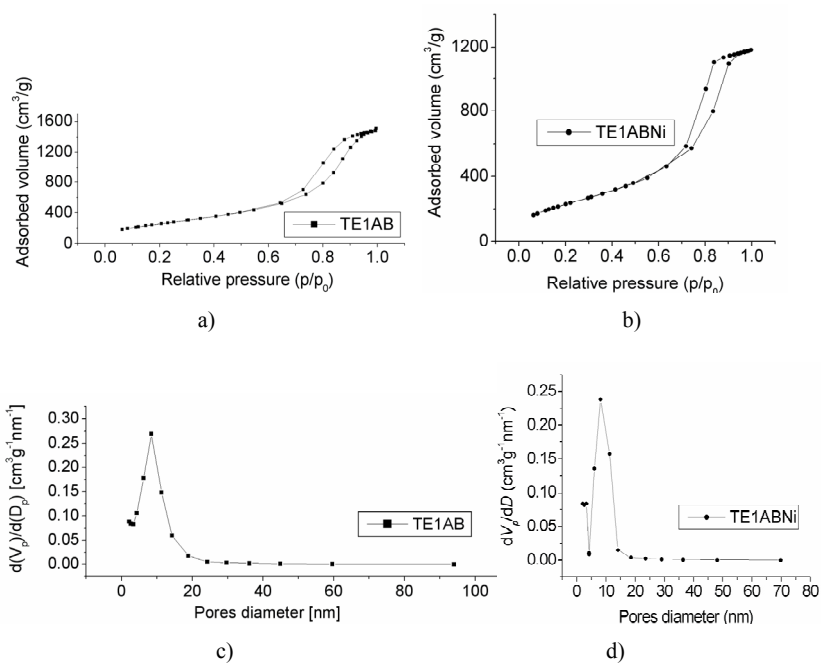


Fig. 1 – Nitrogen adsorption-desorption isotherms and pore size distribution.

X-ray powder diffraction patterns of the samples were recorded in order to identify the crystalline phase formed in the nanocomposites. At small 2θ angles, the baseline presents a broad maximum around 22-24°, which corresponds to an amorphous signal of the silica matrix. In the case of TE1ABNi XRD pattern,

(Fig. 2a), the four observed peaks corresponding to Miller indices (111), (200), (220) and (311) was assigned metallic nickel face-centered cubic type (Fm3m space group) (JCPDS 4-850) [38]. No nickel oxide signals appeared in the XRD pattern. The main diffraction lines observed in TE1ABFe X-ray diffraction pattern, (Fig. 3a) are attributable, without any doubt, to a cubic iron oxide spinel phase. But, at this point, one cannot make any accurate distinction between maghemite or magnetite phases. Further investigations, as Mössbauer spectroscopy and electron diffraction (data not shown), have proved that the identified iron oxide spinel phase is  $\gamma$ -Fe<sub>2</sub>O<sub>3</sub>. The XRD experimental pattern of the TE1ABNiFe nanocomposite aerogel sample derived from silica gel impregnated with both Fe and Ni precursors (Fig. 4a) shows that beside spinel nickel ferrite lines also metallic nickel diffraction features are present. In transmission electron microscopy (TEM images) (Figs. 2b, 3b and 4b, respectively) well defined spherical particles, which are relatively homogeneously dispersed in the silica matrix, were observed. The particles average diameter values of the synthesized aerogel samples are also given in Table 1.

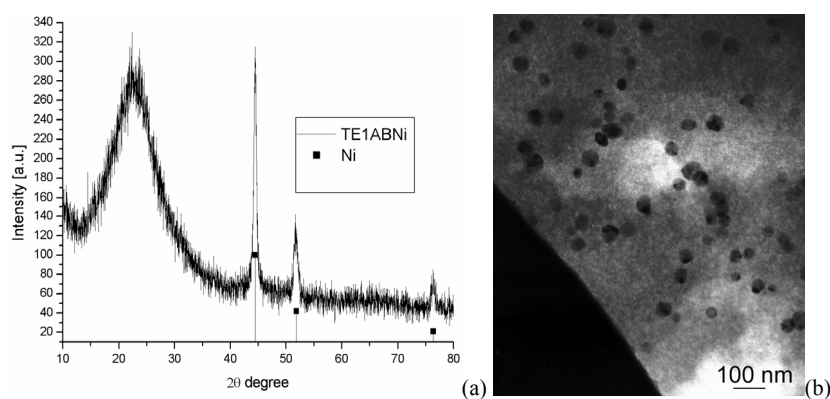


Fig. 2 – X-ray diffraction (a) and TEM photograph (b) of the TE1ABNi aerogel.

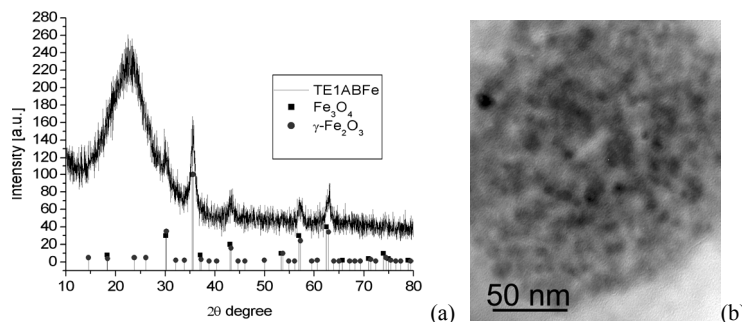


Fig. 3 – X-ray diffraction (a) and TEM photograph (b) of the TE1ABFe aerogel.

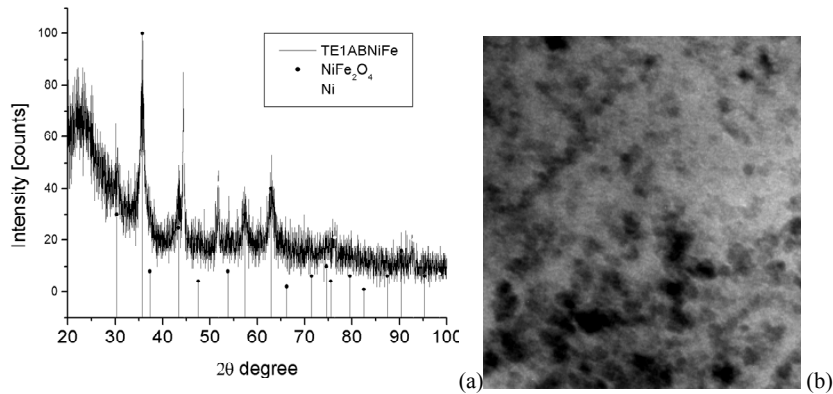


Fig. 4 – X-ray diffraction (a) and TEM photograph (b) of the TE1ABFe aerogel.

In Figs. 5, 6 and 7 respectively, the ambient temperature magnetization curves of the TE1ABNi, TE1ABFe and TE1ABNiFe aerogel nanocomposite samples, are shown.

The VSM measurements, at room temperature, indicate that the TE1ABNi aerogel nanocomposite sample exhibits ferromagnetic behavior with characteristic parameters as saturation magnetization ( $M_s$ ) of 2.84 emu/g and coercivity ( $H_c$ ) of 100 Oe. Taking into account that the nanocomposite sample contains 6 wt. % Ni, the calculated value of the saturation magnetization of Ni was 47.3 emu/g, that is nearby the reported bulk saturation magnetization of Ni (55.4 emu/g) [39]. This value is also comparable with another evaluated value for a nickel nanoparticles system having similar nanoparticles dimensional range [40].

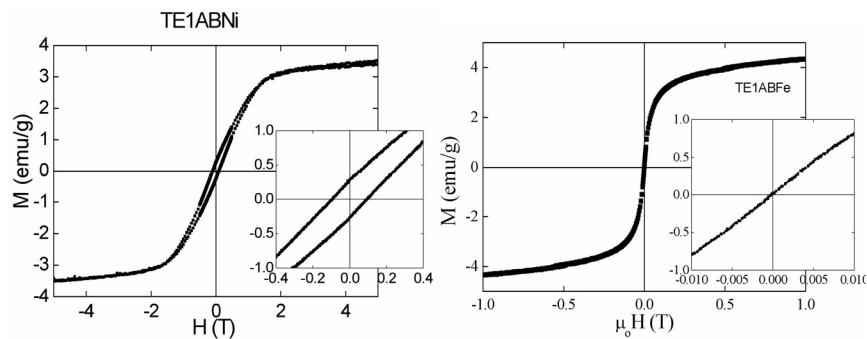


Fig. 5 – VSM magnetization curve of TE1ABNi aerogel.

The TE1ABFe sample magnetic measurement resulted in a saturation magnetization value of 3.8 emu/g and zero coercivity that confirms a superparamagnetic behavior at room temperature of the obtained nanocomposite.

The calculated saturation magnetization corresponding to  $\gamma$ -Fe<sub>2</sub>O<sub>3</sub> concentration in the nanocomposite sample has a value of 44.3 emu/g (which is higher than those reported for maghemite nanoparticles systems of similar sizes, prepared by different other routes) [31, 41].

As shown in Fig. 6, TE1ABNiFe aerogel nanocomposite sample displays mainly superparamagnetic behavior at room temperature with a very low coercivity value (25 Oe).

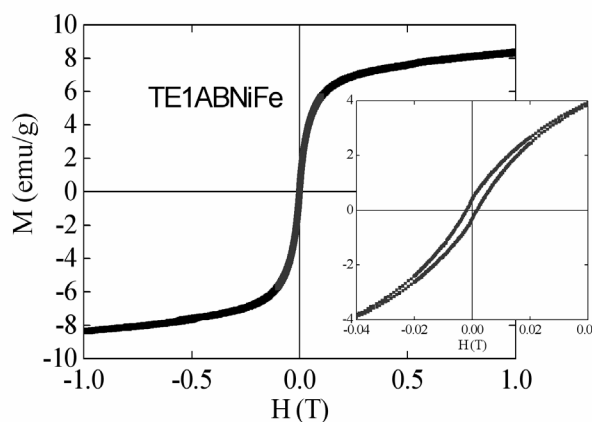


Fig. 6 – VSM magnetization curve of TE1ABNiFe aerogel.

#### 4. CONCLUSIONS

A two step acid-base catalysed sol-gel processing resulted in formation of monolithic silica gels. After impregnation with metallic ( $\text{Ni}^{2+}$ ,  $\text{Fe}^{2+}$ ) ethanol solution and evacuation of solvent in supercritical conditions, monolithic aerogel nanocomposites were directly obtained. No further post-annealing treatments were required to obtain crystalline phases. These phases are: face-centered cubic metallic nickel (in Ni/silica aerogel nanocomposite sample), cubic  $\gamma$ -Fe<sub>2</sub>O<sub>3</sub> (in Fe/silica aerogel nanocomposite sample), as well as cubic spinel nickel ferrite along metallic nickel (in (Ni,Fe)/silica aerogel nanocomposite sample).

Metallic oxide/silica aerogel nanocomposite samples (either maghemite or nickel ferrite) presented superparamagnetic behaviour at room temperature, with zero coercive field (in the case of  $\gamma$ -Fe<sub>2</sub>O<sub>3</sub>) and very low coercivity (25 Oe in the case of nickel ferrite).

Ni/silica aerogel nanocomposite sample (6 wt. % Ni) exhibited room temperature ferromagnetic magnetic properties. The obtained value of the

saturation magnetization, 47.3 emu/g, is comparable with both reported values of nickel bulk and nickel nanoparticle similar systems.

*Acknowledgements.* We thank dr. Anna Roig and dr. Elies Molins from Institut de Ciència de Materials de Barcelona, for the X-ray diffraction and Mössbauer spectroscopy measurements and dr. Josep Nogues from Institutio Catalana de Recerca i Estudis Avancats (ICREA) – Spain for VSM measurements.

## REFERENCES

1. B. Martinez, A. Roig, X. Obradors, E. Molins, A. Rouanet, C. Monty, Magnetic properties of  $\gamma$ -Fe<sub>2</sub>O<sub>3</sub> nanoparticles obtained by vaporization condensation in a solar furnace, *J. Appl. Phys.*, **79**, 5, 2580–2586 (1996)
2. E. M. Chudnovsky, L. Gunther, Quantum theory of nucleation in ferromagnets, *Phys. Rev. B*, **37**, 9455–9459 (1988)
3. C. C. Berry, A. S. G. Curtis, Functionalisation of magnetic nanoparticles for applications in biomedicine *J. Phys. D: Appl. Phys.* **36** (13), R198-R206, (2003)
4. Y.P. He, S.Q. Wang, C. R. Li, Y.M. Miao, Z. Y. Wu, B. S. Zou, Synthesis and characterization of functionalized silica-coated Fe<sub>3</sub>O<sub>4</sub> superparamagnetic nanocrystals for biological applications, *J. Phys. D: Appl. Phys.* **38** (9), 1342-1350 (2005)
5. J.K. Ruuge, A.N. Ruzetski, Magnetic fluids as drug carriers: Targeted transport of drugs by a magnetic field, *J Magn Magn. Mater.* **122**, 1–3, 335–339 (1993)
6. N.M. Pope, R.C. Alsop, Y.A. Chang, A.K. Smith, Evaluation of magnetic alginate beads as a solid support for positive selection of CD34+ cells, *J. Biomed. Mat. Res.* **2**, 449–457, (1994)
7. M.R. Zachariah, M.I. Aquino, R.D. Shull, E.B. Steel, Formation of superparamagnetic nanocomposites from vapor phase condensation in a flame, *Nanostruct. Materials*, **5**, 383-392, 1995
8. B.H. Sohn, R.E. Cohen, G.C. Papaefthymiou, Magnetic Properties of Iron Oxide Nanoclusters within Microdomains of Block Copolymers, *J. Magn.Magn. Mater.* **182**, 216–224, 1998
9. Z. Y. Zhong, Z. T. Xiong, L. F. Sun, J. Z. Luo, P. Chen, X. Wu, J. Lin, K. L. Tan, Nanosized Nickel(or Cobalt)/Graphite Composites for Hydrogen Storage, *J. Phys. Chem. B*, **106**, 9507–9513, (2002).
10. G.H. Lee, S.H. Huh, J.W. Jeong, H.-C. Ri, Excellent magnetic properties of fullerene encapsulated ferromagnetic nanoclusters, *J. of Magn. Magn. Mater.* **246**, 404–411, (2002).
11. J.S. Jung, K.-H. Choi, W.-S. Chae, Y.-R. Kim, J.-H. Jun, L. Malkinski, T. Kodendath, W. Zhou, J. B. Wiley, C. J. O'Connor, Synthesis and characterization of Ni magnetic nanoparticles in AlMCM41 host, *J. Phys. Chem. Solids*, **64**, 385–390 (2003).
12. D.J. Suh, T.-J. Park, J.-H. Kim, Nickel–alumina aerogel catalysts prepared by fast sol–gel synthesis, *J. Non-Crystalline Solids*, **225**, 168–172, (1998).
13. S. Krompiec, J. Mrowiec-Białon, K. Skutil, A. Dukowicz, L. Pajak, A.B. Jarzebski, Nickel–alumina composite aerogel catalysts with a high nickel load: a novel fast sol–gel synthesis procedure and screening of catalytic properties, *J. Non-Cryst. Solids*, **315**, 297–303, (2003).
14. S.-H. Lee, D.J. Suh, T.-J. Park K.-L. Kim, The effect of heat treatment conditions on the textural and catalytic properties of nickel–titania composite aerogel catalysts, *Catalysis Communications*, **3**, 441–447, (2002).
15. G. Ennas, A. Mei, A. Musinu, G. Piccaluga, G. Pinna, S. Solinas, Sol–gel preparation and characterization of Ni–SiO<sub>2</sub> nanocomposites, *J. Non-Cryst. Solids*, **232–234**, 587–593, (1998).

16. H. Nathani, R.D.K. Misra, Surface effects on the magnetic behavior of nanocrystalline nickel ferrites and nickel ferrite-polymer nanocomposites, *Materials Science and Engineering B* 113, 228–235, (2004).
17. X. Huang, Z. Chen, A study of nanocrystalline NiFe<sub>2</sub>O<sub>4</sub> in a silica matrix, *Materials Research Bulletin* 40 (2005) 105–113.
18. T. Lutz, C. Estournes, J.L. Guille, Metal (Fe, Co, Ni) Nanoparticles in Silica Gels: Preparation and Magnetic Properties, *Journal of Sol-Gel Science and Technology*, 13, 929-932 (1998)
19. M.C.Hobson, Jr., H.M.Gager, *Journal of Catalysis*, A Mössbauer effect study on crystallites of supported ferric oxide, 16, 254–263 (1970).
20. A.C. Pierre, G.M. Pajonk, Chemistry of Aerogels and Their Applications, *Chem. Rev.* 102, 4243–4266 (2002).
21. Ll.Casas, A. Roig, E. Rodriguez, E. Molins, J. Tejada, J. Sort, Silica aerogel–iron oxide nanocomposites: structural and magnetic properties *Journal of Non-Crystalline Solids*, 285, (1-3), 37–43 (2001).
22. P. Fabriziooli, T. Burgi, M. Burgener, S. van Doorslaer, A. Baiker, Synthesis, structural and chemical properties of iron oxide–silica aerogels *J. Mater. Chem.*, 12, 619–630 (2002).
23. M. Gich, Ll. Casas, A. Roig, E. Molins, J. Sort, S. Suriñach, M. D. Baró, J. S. Muñoz, L. Morellon, M. R. Ibarra, J. Nogués, High-coercivity ultralight transparent magnets, *Appl. Phys. Lett.*, 82, 4307–4309 (2003).
24. N. Leventis, I. A. Elder, G. J.Long, D. R.Rolison, Using Nanoscopic Hosts, Magnetic Guests, and Field Alignment to Create Anisotropic Composite Gels and Aerogels, *Nano Lett.*, 2, 63–67 (2002).
25. H. H.Hamdeh, J.C. Ho, S.A. Oliver, R.J. Willey, G. Oliveri, G. Busca, Magnetic properties of partially-inverted zinc ferrite aerogel powders, *J. Appl. Phys.*, 81, 1851–1857(1997).
26. C. Cannas, M.F. Casula, G. Concas, A. Corrias, D. Gatteschi, A. Falqui, A. Musinu, C. Sangregorio, G. Spano, Magnetic properties of  $\gamma$ -Fe<sub>2</sub>O<sub>3</sub>–SiO<sub>2</sub> aerogel and xerogel nanocomposite materials, *J. Mater. Chem.*, 11, 3180–3187 (2001).
27. M.R. Ayers, X.Y. Song, A.J. Hunt, Preparation of Nanocomposite Materials Containing WS<sub>2</sub>, d-WN, Fe<sub>3</sub>O<sub>4</sub>, or Fe<sub>9</sub>S<sub>10</sub> in a Silica Aerogel Host. *J. Mater. Sci.*, 31 6251–6257 (1996).
28. M.F.Casula, A.Corrias, G. Paschina, Iron oxide–silica aerogel and xerogel nanocomposite materials, *J. Non-Cryst. Solids*, 293–295 25–31 (2001).
29. Ll. Casas, A.Roig, E. Molins, J.M. Greneche, J. Asenjo, J. Tejada, Iron oxide nanoparticles hosted in silica aerogels, *Appl. Phys. A*, 74 591–597 (2002).
30. K. Racka, M. Gich, A. Slawska-Waniewska, A. Roig, E. Molins, Magnetic properties of Fe nanoparticle systems, *J. Magn. Mater.* 290–291, 127–130 (2005).
31. F. Bentivegna, J. Ferré, M. Nyvlt, J.P. Jamet, D. Imhoff, M. Canva A. Brun, P. Veillet, S. Visnovsky, F. Chaput, J. P. Boilot, Magnetically textured  $\gamma$ -Fe<sub>2</sub>O<sub>3</sub> nanoparticles in a silica gel matrix: Structural and magnetic properties, *Journal of Applied Physics* 83, 12, 7776–7788 (1998).
32. F. Del Monte, M.P. Morales, D. Levy, A. Fernandez, M. Ocana, M.A. Roig, E. Molins, E.K. O’Grady, and C.J. Serna, Formation of  $\gamma$ -Fe<sub>2</sub>O<sub>3</sub> Isolated Nanoparticles in a Silica Matrix, *Langmuir*, 13, 3627–3634 (1997).
33. C. Cannas, D. Gatteschi, A. Musinu, G. Piccaluga, C. Sangregorio, Structural and Magnetic Properties of Fe<sub>2</sub>O<sub>3</sub> Nanoparticles Dispersed over a Silica Matrix, *J. Phys. Chem.*, 102, 7721–7726 (1998).
34. G. Schemer, G. Markovich, Enhancement of Magneto-Optical Effects in Magnetite Nanocrystals Near Gold Surfaces *J. Phys. Chem. B*, 106, 9195–9197 (2002).
35. Y. Lu, Y. Yin, B.T. Mayers, Y. Xia, Modifying the Surface Properties of Superparamagnetic Iron Oxide Nanoparticles through A Sol-Gel Approach, *Nano Lett.*, 2 183–186 (2002).

36. M. Popovici, M. Gich, A. Roig, L. Casas, E. Molins, C. Savii, D. Becherescu, J. Sort, S. Surinach, J.S. Munoz, M.D. Baro, J. Nogues, Ultraporous Single Phase Iron Oxide-Silica Nanostructured Aerogels from Ferrous Precursors *Langmuir*, 20(4), 1425–1429 (2004).
37. S.J. Gregg, K.S.W. Sing, *Adsorption, Surface Area and Porosity*, Academic, London, 1982.
38. JCPDS 4-850, *Natl. Bur. Stand. (US)*, Circ. 539, Vol. 0, 1953, 13.
39. H.P.J. Wijn, Ed. *Magnetic Properties of Metals: d-elements, alloys and Compounds*, Springer Verlag Berlin Heidelberg, 1991, p. 7.
40. X. Sun, A. Gutierrez, M.J. Yacaman, X. Dong, S. Jin, Investigations on magnetic properties and structure for carbon encapsulated nanoparticles of Fe, Co, Ni, *Materials Science and Engineering A*, 286, 157–160 (2000).
41. M. Nogami, Asuha, Preparation of  $\gamma$ -Fe<sub>2</sub>O<sub>3</sub> – containing silica glasses by the sol-gel process, *Journal of Materials Science Letters*, 12, 1705–1707 (1993).